MATSIM: Development of a Voxel Model of the MATROSHKA Astronaut Dosimetric Phantom

Peter Beck, *Member, IEEE*, Andrea Zechner, Sofia Rollet, Thomas Berger, Robert Bergmann, Michael Hajek, Christian Hranitzky, Marcin Latocha, Günther Reitz, Hannes Stadtmann, Norbert Vana, and Michael Wind, *Member, IEEE*

***Abstract*—The AIT Austrian Institute of Technology coordinates the project MATSIM (MATROSHKA Simulation) in collaboration with the Vienna University of Technology and the German Aerospace Center, to perform FLUKA Monte Carlo simulations of the MATROSHKA numerical phantom irradiated under reference radiation field conditions as well as for the radiation environment at the International Space Station (ISS). MATSIM is carried out as co-investigation of the ESA ELIPS projects SORD and RADIS (commonly known as MATROSHKA), an international collaboration of more than 18 research institutes and space agencies from all over the world, under the science and project lead of the German Aerospace Center. During MATSIM a computer tomography scan of the MATROSHKA phantom has been converted into a high resolution 3-dimensional voxel model. The energy imparted and absorbed dose distribution inside the model is determined for various radiation fields. The major goal of the MATSIM project is the validation of the numerical model under reference radiation conditions and further investigations under the radiation environment at ISS. In this report we compare depth dose distributions inside the phantom measured with thermoluminescence detectors (TLDs) and an ionization chamber with FLUKA Monte Carlo particle transport simulations due to ^{60}Co photon exposure. Further reference irradiations with neutrons, protons and heavy ions are planned. The fully validated numerical model MATSIM will provide a perfect tool to assess the radiation exposure to humans during current and future space missions to ISS, Moon, Mars and beyond.**

***Index Terms*—FLUKA Monte Carlo simulation, MATROSHKA dosimetric phantom, space dosimetry, voxel model.**

Manuscript received September 13, 2009; revised April 16, 2010 and May 16, 2010; accepted May 20, 2010. Date of publication July 05, 2011; date of current version August 17, 2011. This work was supported in part by the Austrian Ministry of Traffic, Innovation, and Technology through the Austrian Space Application Programme (ASAP).

P. Beck, S. Rollet, M. Latocha, and M. Wind are with the Austrian Institute of Technology, 1220 Vienna, Austria (e-mail: peter.beck@ait.ac.at; sofia.rollet@ait.ac.at; marcin.latocha@ait.ac.at; michael.wind@ait.ac.at).

A. Zechner is with the Austrian Institute of Technology, 1220 Vienna, Austria, and also with Graz University of Technology, 8010 Graz, Austria (e-mail: andrea.zechner@ait.ac.at).

T. Berger and G. Reitz are with the German Aerospace Center, Institute of Aerospace Medicine, D-51147 Cologne, Germany (e-mail: thomas.berger@dlr.de; guenther.reitz@dlr.de).

R. Bergmann, M. Hajek, and N. Vana are with the Institute of Atomic and Subatomic Physics, Department of Radiation Physics, Vienna University of Technology, A-1020 Vienna, Austria (e-mail: bergmann@ati.ac.at; mhajek@ati.ac.at; vana@ati.ac.at).

C. Hranitzky and H. Stadtmann are with the Dosimetry Laboratory, Seibersdorf Labor GmbH, 2444 Seibersdorf, Austria (e-mail: christian.hranitzky@seibersdorf-laboratories.at; hannes.stadtmann@seibersdorf-laboratories.at).

Color versions of one or more of the figures in this paper are available online at http://ieeexplore.ieee.org.

Digital Object Identifier 10.1109/TNS.2011.2157704

I. Introduction

The International Space Station (ISS) provides significant challenges for radiation protection of the crew due to the extended duration of missions, the exceptionally dynamic nature of the radiation environment in ISS orbit, and the necessity for numerous extravehicular activities (EVA) for station construction and maintenance [1].

Although considerable dosimetric data have been accumulated from several spaceflight experiments [2]–[14], it is not yet possible to provide a full quantitative description of all the relevant radiation field parameters. In order to assess the radiation load that astronauts are exposed to during intra- and extravehicular activities, the MATROSHKA facility has been developed [15]–[17], [19]. MATROSHKA is an ESA facility under the scientific and project lead of DLR. Several thousand TLDs are applied to measure the depth dose distribution within an anthropomorphic phantom exposed in- and outside the ISS [18]–[20]. Besides the TLDs the phantom also houses active and passive radiation detectors in specified organ positions for the determination of the organ dose equivalent. The main goals of the MATROSHKA experiment are long-term depth dose measurements at various locations in and outside the ISS including the determination of the neutron contribution, organ and skin doses and Monte Carlo transport code verification for the calculation of the dose distribution inside the phantom.

The AIT Austrian Institute of Technology coordinates the project MATSIM (MATROSHKA Simulation) in collaboration with the Vienna University of Technology (ATI) and the German Aerospace Center (DLR) to perform Monte Carlo simulation of high energy radiation particle transport inside the MATROSHKA phantom.

The main aim of the project MATSIM is the development and validation of a numerical simulation model of the MATROSHKA phantom. The fully validated MATSIM model will provide comprehensive risk assessment of radiation hazard to humans in space. MATSIM will provide prediction of tissue and organ doses and the estimation of radiation risk for human missions under diverse exploratory conditions such as future missions to ISS, Moon, and Mars. Furthermore, it will provide valuable information for optimization of spacecraft shielding design and personal dosimeter developments for mixed radiation fields.

The innovative part of the MATISM project is the validation of the MATSIM model by a tremendous set of measurements under well defined reference radiation fields. In this paper we describe the development of the 3-dimensional voxel

Fig. 1. Left: Inside view of the MATROSHKA phantom head (slice #3) housing active and passive eye detectors. Right: Cut through the head (slice #2) with passive TLDs. (Credit DLR).

model based on computer tomography (CT) scans of the MATROSHKA phantom, used for ground based experiments. The numerical modeling and the simulations are done with the FLUKA Monte Carlo particle transport code. Comparisons between TLD, ionization chamber measurements and simulations of absorbed dose in water inside the phantom due to exposure to ^{60}Co photon reference fields are described. Further measurements in well defined neutron fields are planned and will be presented in a next paper. The validated numerical model will then be exposed to the simulated radiation field in low-earth orbit and the dose distribution within the torso will be compared with the actual measurements done on board of ISS. As an example, in this paper a simulation of the energy density inside the numerical phantom irradiated with the proton field expected at ISS position is also described.

II. MATROSHKA Phantom

The anthropomorphic phantom used in the MATROSHKA experiment is onboard the ISS is a RANDO upper torso made of a natural human skeleton embedded in tissue equivalent material (polyurethane) simulating soft and muscle tissue [19]–[21]. The phantom is 40 cm wide, 85 cm high and it is cut into 33 slices with the thickness of 25.4 mm each. It is attached to a base structure, where the electronics is accommodated [19], [20], [22]. A picture of the phantom head is shown in Fig. 1. A summary data of the ground MATROSHKA phantom (similar to the one exposed onboard the ISS) is given in Table I.

In each slice long horizontal holes (see Fig. 2) are drilled to accommodate up to about 4800 TLDs used to measure the absorbed dose distribution inside the phantom. The dosimeters are hold together in polyethylene tubes inserted in the drilled channels. A total number of 11 different types of TLDs are used to determine the exposure within MATROSHKA. The TLDs vary in material (CaF_2, LiF), in their Lithium enrichment (^{6}Li and ^{7}Li), in their dopants (Mg, Cu, P; Mg, Ti, and Tm) and in their density and also in their shapes: rectangular ($3.2 \times 3.2 \times 0.6$ mm^3 or $3.2 \times 3.2 \times 0.9$ mm^3) and cylindrical (4.5 mm diameter and 0.6 mm height).

For selected organs such as eyes, lungs, stomach, kidney and intestine, so called organ dose boxes (see Fig. 2) housing active silicon dosimeters and passive dosimeters are applied. The active and passive dosimeters were prepared, inserted and, subsequently, read out by different experimental groups. Further details to MATROSHKA and detectors are given in reference [18]–[23].

TABLE I
Data of the MATROSHKA Ground Torso and Ground Head Phantom and the Matsim Torso and Matsim Head

	Torso	**Head**
height	H = 85 cm	h= 30 cm
maximal width	w_{max} = 40 cm	w_{max} = 25 cm
maximal depth	d_{max} = 22 cm	d_{max} = 22 cm
materials	bones, TE plastic	bones, TE plastic
number of slices	33	10
slice thickness	25.4 mm	25.4 mm
number of TLDs	840	104
simulated organs	eyes, lung, stomach, kidney, intestine	eyes
CT-scan pixel resolution	512 × 512 × 278	360 × 565 × 486
total number of voxels	$7.3 \cdot 10^7$	$9.9 \cdot 10^7$
voxel size (mm)	0.8 × 0.8 × 3.1	0.6 × 0.4 × 0.6

Fig. 2: Left: passive TLDs in the intestine (slice #27) and cut outs for active and passive organ dose boxes. Right: typical design of an organ dose box used for passive detectors. (Credit DLR).

III. Numerical Modeling

The numerical modeling and the simulations are done with the FLUKA Monte Carlo particle transport code. The FLUKA code simulates the interaction and propagation of particles such as photons and electrons in a wide energy range from 1 keV to thousands of TeV, hadrons up to 20 TeV and all the corresponding antiparticles, neutrons down to thermal energies, and heavy ions [24]. Since the 2006.3 release, FLUKA provides the possibility to describe a complex geometry in terms of voxels [25]. This functionality of FLUKA was used to transfer the MATROSHKA CT-scans into a full geometry description.

Two CT scans, one of the MATROSHKA ground phantom torso and one of the head were performed by DLR at the "Strahleninstitut Köln" in Cologne, Germany (see Fig. 3 and Fig. 4).

The CT scan gives a matrix containing information about the local electron density distribution in the phantom based on the Hounsfield scale. The phantom's material assignment was determined by grouping these values into classes resulting in the model geometry to be used as input in the FLUKA Monte Carlo code. The detectors were put inside the foreseen cut-outs by a software code developed at AIT. The material composition of the TLD detectors in the numerical model is Lithium Fluoride (LiF), whereas natural Lithium is used.

A total number of $7.3 \cdot 10^7$ voxels is used to reconstruct the scan of the entire MATROSHKA torso and $9.9 \cdot 10^7$ voxels for

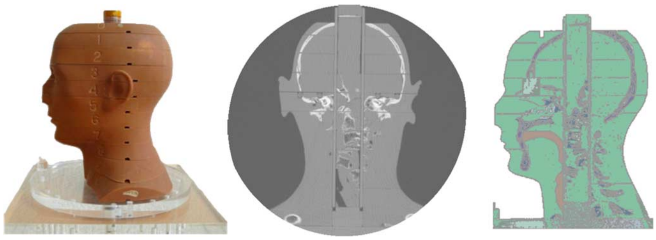

Fig. 3: From left to right: MATROSHKA ground phantom head, CT-scan of the same phantom and the phantom's voxel geometry MATSIM-Head for input in the FLUKA Monte Carlo code.

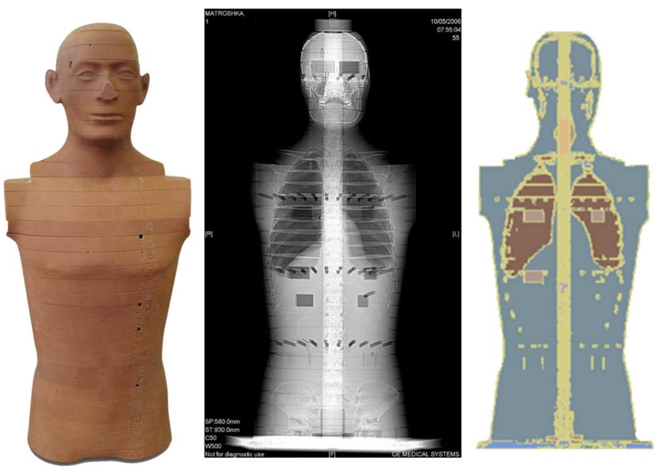

Fig. 4: From left to right: MATROSHKA phantom torso, computer tomography of the phantom and the phantom's voxel geometry MATSIM-Torso v1.1, for input in the FLUKA Monte Carlo code.

the phantom head, respectively. A data summary of the MATROSHKA ground phantom and the MATSIM model is given in Table I. Pictures of the simulation geometries MATSIM head and MATSIM torso are given in Fig. 3 and Fig. 4.

IV. Measurements and Simulations

Measurements under well defined radiation reference conditions with the phantom head, provided by DLR, were carried out in the radiation standard laboratory of the Seibersdorf Labor GmbH (a company of the AIT Austrian Institute of Technology), to verify the developed numerical model. The phantom head was exposed to ^{60}Co photons. Measurements were performed with thermoluminescence dosimeters and an ionization chamber type 31013 PTW [26]. The TLDs as well as the ionization chamber are calibrated in terms of absorbed dose in water D_{W}. The TLDs were packed in stacks of four (two dosemeters of type TLD-600 and TLD-700 [23], respectively). The size of a TLD stack is $3.2 \times 3.2 \times 3.6$ mm. The detector stacks were inserted in tubes separated by polyethylene spacers and placed at 26 measurement positions in the foreseen cut-outs of slice #4. Each measurement position is defined by a code within a horizontal and vertical grid of 2.5 cm (see Fig. 5). The TLDs are located in the tubes A-H. The results are expressed as the mean value of the four TLDs per position, each with a measurement uncertainty of 7% (1σ).

The ionization chamber was located in the rod center in slice #2, and in the eye box (slices #3). The phantom head was irradiated a) with a multi-directional ^{60}Co photon beam incidence between 0° and 330° in 30 degree steps and b) with mono-directional beam incidence frontal (0°) (see Fig. 5).

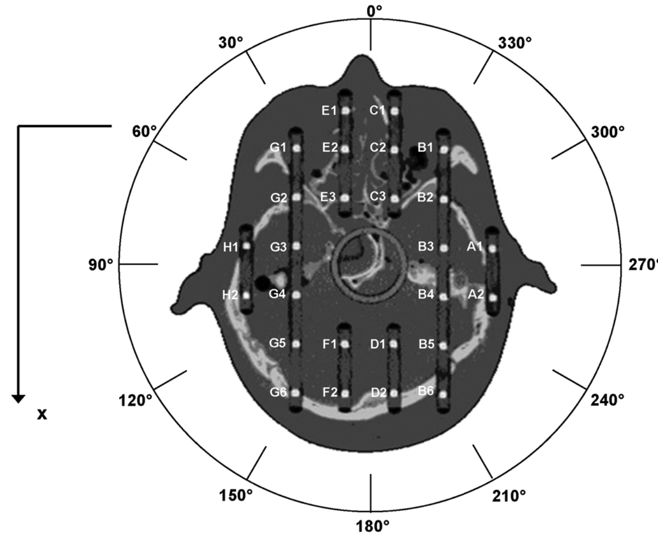

Fig. 5. Irradiation set-up of the MATROSHKA phantom head and TLD position coding in slice #4.

The reference irradiation point is in the center of the rod, within slice#5. The relative dose deviation within a field size of 27×27 cm^2, that covers the entire MATROSHKA head, is less than 3% compared to the reference values in the center. At a distance of 450 cm between the source and the reference point, the reference dose given in air kerma, K_{A} was determined to be 200 mGy, with an air kerma rate of 574 ± 11 mGy/h.

Simulations were performed with the numerical model of the MATROSHKA head exposed to ^{60}Co photons. The simulations provide energy imparted in LiF at the TLD detector positions. By dividing the energy imparted by the detector mass, absorbed dose in LiF is obtained. A comparison of simulated kerma and absorbed dose values shows that secondary electron equilibrium exists at each detector position. Therefore a conversion factor of 1.2 can be used to converting absorbed dose in LiF to water. This factor is obtained by taking the ratio of the mass energy absorption coefficients of LiF and water for 1.25 MeV photons energy [29].

The statistical uncertainties on the simulation values are $<1\%$. Further sources of uncertainties are the photon cross sections used in the simulation code, the conversion factor of absorbed dose in LiF to water, and the photon source description. Additionally to the statistical uncertainty of the simulation of 1% the systematic uncertainties are assessed to 7% to get an overall uncertainty in the order of 8%.

In the following, results of TLD and ionization chamber measurements and simulations are presented.

V. Results and Discussion

In Table II the results for the detector measurements and simulations in terms of absorbed dose in water are given together with their ratio.

Fig. 6 and Fig. 7 show the TLD and IC measurements of the absorbed dose D_{W} in the MATROSHKA head due to ^{60}Co mono- and multi-directional irradiation, respectively.

TABLE II
TLD and IC Measurements and Simulations of Absorbed Dose in Water D_W Due to Mono- and Multi-Directional ^{60}Co Irradiation. The Ratio Between Measurements and Simulation Values Are Also Given. Measurement Uncertainty (1σ) of TLD: 7%, IC: 3%, and Simulations 8%

Detector Position	Absorbed dose in water D_w (mGy)				Ratio	
	Measurements		Simulations		Meas / Sim	
	Beam Incidence					
	Mono	Multi	Mono	Multi	Mono	Multi
IC rod slice #2	159.0	166.1	162.5	170.5	0.98	0.97
IC eye	219.8	-	213.0	-	1.03	-
TLD slice #4						
A1	195.7	176.1	196.4	172.4	1.00	1.02
A2	194.6	164.5	180.7	170.5	1.08	0.96
B1	205.9	169.2	205.2	170.3	1.00	0.99
B2	189.8	164.2	187.5	167.0	1.01	0.98
B3	163.8	159.5	161.7	162.5	1.01	0.98
B4	139.2	161.8	151.5	163.7	0.92	0.99
B5	135.1	169.7	129.9	162.6	1.04	1.04
B6	116.5	162.0	111.2	169.6	1.05	0.96
C1	221.7	166.6	205.3	166.9	1.08	1.00
C2	201.3	164.5	203.9	165.8	0.99	0.99
C3	185.2	155.0	175.1	160.6	1.06	0.97
D1	140.8	164.4	138.4	160.4	1.02	1.02
D2	119.4	163.4	117.9	164.9	1.01	0.99
E1	233.4	161.9	202.6	171.2	1.15	0.95
E2	204.2	153.1	191.1	159.1	1.07	0.96
E3	181.8	154.9	163.1	160.8	1.11	0.96
F1	141.7	153.0	116.0	157.9	1.22	0.97
F2	110.4	160.9	101.0	159.5	1.09	1.01
G1	206.1	160.9	198.6	166.5	1.04	0.97
G2	176.2	163.0	200.9	161.3	0.88	1.01
G3	166.9	156.3	156.8	163.6	1.06	0.96
G4	154.1	160.4	150.0	160.4	1.03	1.00
G5	128.1	162.0	131.6	164.4	0.97	0.99
G6	111.9	163.7	114.8	168.5	0.97	0.97
H1	178.2	159.6	177.1	166.3	1.01	0.96
H2	149.4	163.5	161.0	167.6	0.93	0.98

In case of mono-directional beam incidence the absorbed dose decreases from front to back of the phantom head by a factor of 2. For the multi-directional exposure the TLD measurements show a constant behavior from the front to the back as well as from left to right side which is expected for a multi-directional irradiation case. The IC measurements are comparable with TLD results in their vicinity.

For mono-directional irradiation the IC measurement gives an absorbed dose value of 220 ± 4 mGy in the eye and 159± 3 mGy in the rod. The simulated absorbed dose values in the same positions are 213.0 ± 4.3 mGy and 163 ± 3 mGy, respectively. The simulated values agree with the measured ones within one standard deviation in each position.

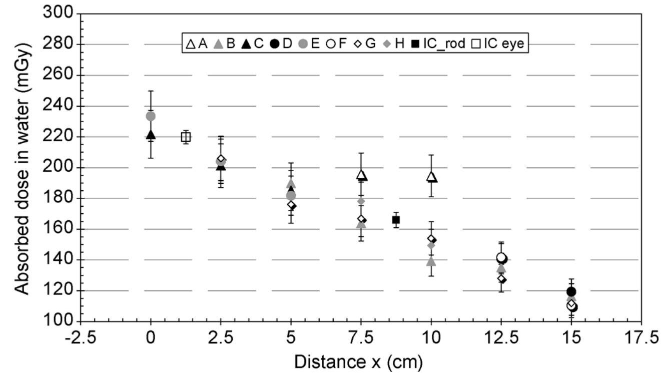

Fig. 6. Measurements of absorbed dose in water, D_W, due to ^{60}Co mono-directional irradiation (MATROSHKA head slice #4; TLDs within tubes A-H and IC measurements in central rod slice #2 and eye box slice#3).

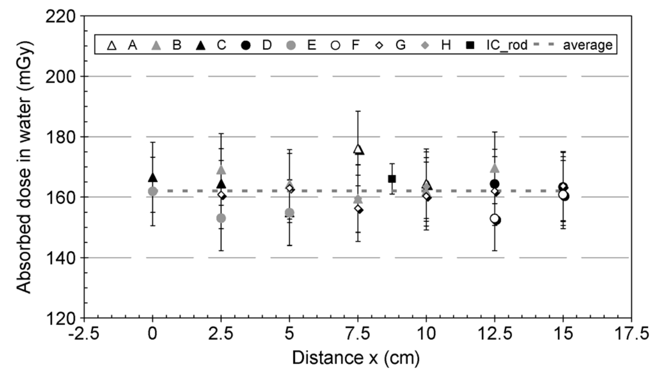

Fig. 7. Measurements of absorbed dose in water, D_W, due to ^{60}Co multi-directional irradiation (MATROSHKA head slice #4, TLDs within tubes A-H and IC in central rod in slice #2).

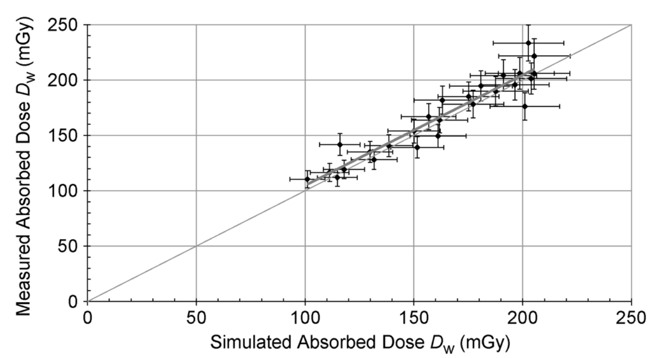

Fig. 8. Correlation between TLD measurement and simulation results of absorbed dose in water, D_W, due to ^{60}Co mono-directional irradiation (MATROSHKA head slice #4).

Fig. 8 shows the correlation between TLD measurements and simulation for the mono-directional irradiation. Considering all TLDs, the correlation coefficient is 0.92, and the mean ratio of measured and simulated results is 1.03. In the case of multi-directional exposure of the MATROSHKA head to ^{60}Co photons the simulated value of the IC (170 ± 3 mGy) agrees within one standard deviation with the measured value (166 ± 5 mGy).

Fig. 9 shows the ratio of TLD and ionization chamber measurements with the simulations for multi-directional exposure of the MATROSHKA head to ^{60}Co photons. Considering all TLDs the mean ratio of measured and simulated results is 0.98.

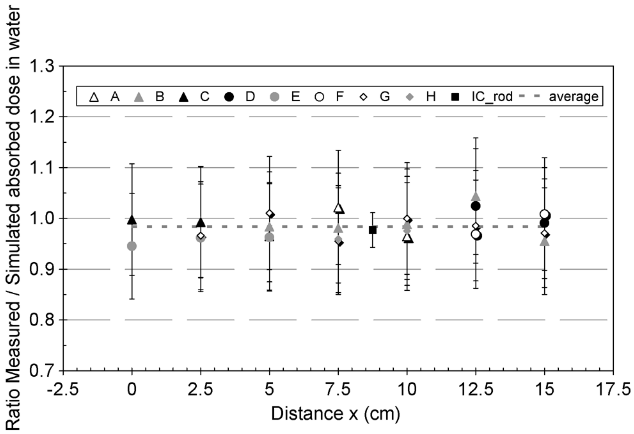

Fig. 9. Ratio between measured and simulated values of absorbed dose in water, D_W, due to ^{60}Co multi-directional irradiation (MATROSHKA head slice #4, TLDs within tubes A-H and IC in central rod in slice #2).

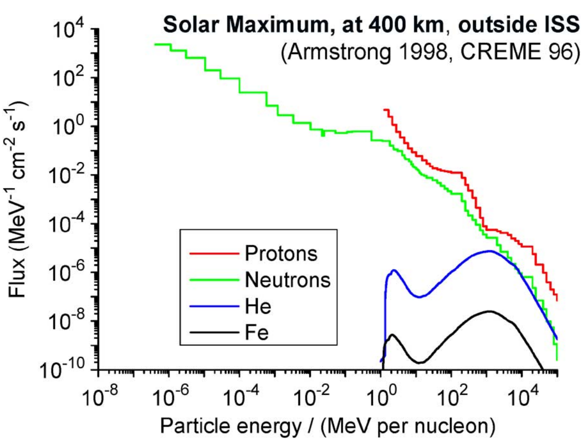

Fig. 10. Proton, neutron, helium and iron particle fluence rate spectra outside the International Space Station (ISS) during solar maximum, at 400 km altitude, 51.6° inclination [27].

VI. Simulation of Proton Exposure

Protons represent the major contribution of absorbed dose in the human body exposed to the radiation environment at the ISS. Fig. 10 shows the fluence spectra of protons, neutrons helium and iron ions giving a significant contribution to the radiation exposure for a position outside the ISS during maximum solar activity at an altitude of 400 km, and an inclination of 51.6°.

The spectral data were taken from the calculations of Armstrong [27] and CREME96 [28]. Scaling factors, published in the same paper [27] were used to convert fluence values from 500 km to 400 km. Simulations of the spatial energy distribution inside the MATSIM torso model due to irradiation by an inward isotropic proton source with the energy spectrum as shown in Fig. 10 are performed and shown in the following.

Fig. 11 shows the density distribution of energy imparted in GeV/cm^3 inside the phantom due to inward irradiation with isotropic protons, outside ISS, during solar maximum conditions, at 400 km altitude and 51.6° inclination (see Fig. 10). It gives a side view of the cross section through the body center, integrated over a thickness of 0.5 cm.

For the same radiation environmental conditions Fig. 12 shows a cross section through the lungs. The integrated thickness is 0.3 cm. It gives the energy imparted density distribution within the lungs and the TLD detectors. The energy imparted within the detectors is significant larger compared to the surrounding tissue material. Fig. 13 shows the density of the energy imparted in GeV/cm^3 inside the lungs, integrated over $0 \leq y \leq 40$ cm as a function of width (along x axis). The energy imparted within the TLD detectors is about 60% higher than in the surrounding tissue. When comparing absorbed dose values the differences between TLD and the surrounding tissue is expected to become smaller. In a further publication we will show absorbed dose values for cross sections of the MATROSHKA phantom and through organs.

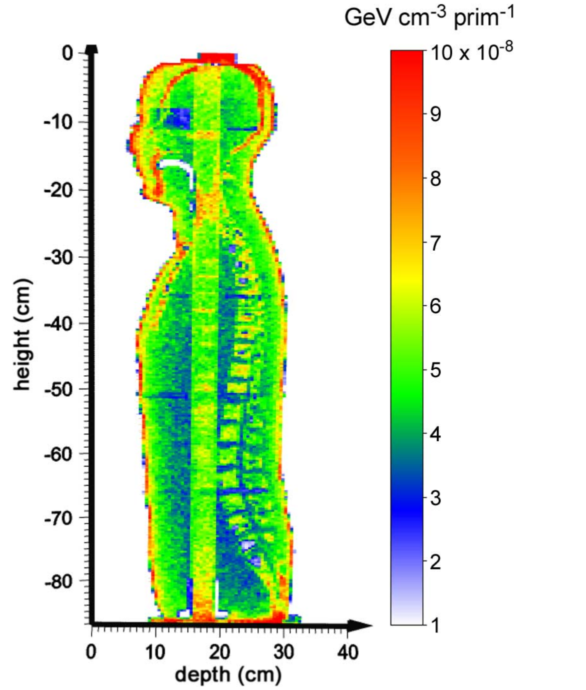

Fig. 11. Density of the energy imparted in GeV/cm3 inside the MATROSHKA phantom due to irradiation with inward isotropic ISS protons. Cross section through the body center; thickness of 0.5 cm.

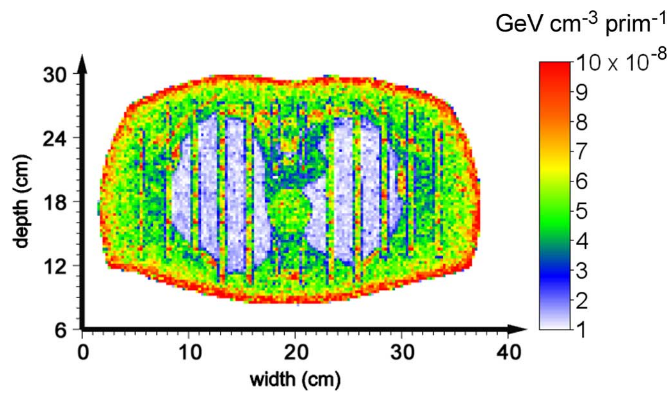

Fig. 12. Density of the energy imparted in GeV/cm^3 inside the lung due to irradiation with inward isotropic ISS protons. Cross section through the lungs; integration thickness 0.3 cm.

VII. Conclusion

The MATSIM torso and head, two numerical voxel models of the dosimetric astronaut phantom MATROSHKA, were de-

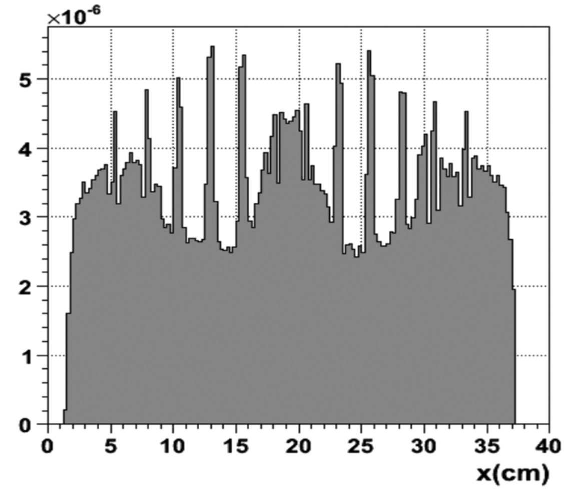

Fig. 13: Density of the energy imparted in GeV/cm^3, integrated over $0 \leq y \leq$ 40 cm as a function of width (along x axis), inside the lungs due to irradiation with inward isotropic ISS protons.

veloped for investigations under reference radiation field conditions and the cosmic radiation environment at ISS. Reference irradiations of the MATROSHKA ground phantom head were carried out with a ^{60}Co source at the radiation standard laboratory in Seibersdorf, Austria. Measurements inside the phantom head were done with TLDs and an ionization chamber. Simulations of the energy imparted due to ^{60}Co irradiation were carried out and absorbed doses were calculated with the Monte Carlo code FLUKA for comparison with the measurements. The simulation results show an excellent agreement with the IC and TLD measurements in each position within the experimental uncertainty (1σ). A first investigation of the simulation of energy imparted due to proton irradiation of the MATSIM torso is carried out. It shows expected high values of energy imparted at the skin, within the bones and the TLD detectors. Further reference irradiation experiments and simulations are planned with neutrons, protons and heavy ions.

REFERENCES

[1] F. A. Cucinotta, M. Shavers, P. B. Saganti, and J. Miller, Eds., Radiation Protection Studies of International Space Station Extravehicular Activity Space Suits, NASA/TP-2003-212051, 2003.

[2] E. R. Benton and E. V. Benton, "Space radiation dosimetry in low-Earth orbit and beyond," *Nucl. Instrum. Methods Phys. Res. Section B*, vol. 184, pp. 255–294, 2001.

[3] G. D. Badhwar, W. Atwell, G. Reitz, R. Beaujean, and W. Heinrich, "Radiation measurements on the MIR Orbital Station," *Radiat. Meas.*, vol. 35, pp. 393–422, 2002.

[4] M. Hajek, T. Berger, N. Vana, M. Fugger, J. K. Pálfalvi, J. Szabó, I. Eördögh, Y. A. Akatov, V. V. Arkhangelsky, and V. A. Shurshakov, "Convolution of TLD and SSNTD measurements during the BRADOS1 experiment onboard ISS (2001)," *Radiat. Meas.*, vol. 43, pp. 1231–1236, 2008.

[5] I. Apáthy, S. Deme, L. Bodnár, A. Csöke, and I. Héjja, "An on board TLD system for dose monitoring on the International Space Station," *Radiat. Prot. Dosim.*, vol. 84, pp. 321–323, 1999.

[6] T. Berger, M. Hajek, L. Summerer, N. Vana, Y. Akatov, V. Shurshakov, and V. Arkhangelsky, "Austrian dose measurements onboard space station Mir and the International Space Station—Overview and comparison," *Adv. Space Res.*, vol. 34, pp. 1414–1419, 2004.

[7] D. O'Sullivan, D. Zhou, E. Semones, W. Heinrich, and E. Flood, "Dose equivalent, absorbed dose and charge spectrum investigation in low Earth orbit," *Adv. Space Res.*, vol. 34, pp. 1420–1423, 2004.

[8] A. B. Akopova, M. M. Manaseryan, A. A. Melkonyan, S. S. Tatikyan, and Y. Potapov, "Radiation measurement on the International Space Station," *Radiat. Meas.*, vol. 39, pp. 225–228, 2005.

[9] G. Reitz, R. Beaujean, E. Benton, S. Burmeister, T. Dachev, S. Deme, M. Luszik-Bhadra, and P. Olko, "Space radiation measurements on-board ISS—The DOSMAP experiment," *Radiat. Prot. Dosim.*, vol. 116, pp. 374–379, 2005.

[10] M. Hajek, T. Berger, M. Fugger, M. Fuerstner, N. Vana, Y. Akatov, V. Shurshakov, and V. Arkhangelsky, "BRADOS—Dose determination in the Russian Segment of the International Space Station," *Adv. Space Res.*, vol. 37, pp. 1664–1667, 2006.

[11] M. Hajek, T. Berger, M. Fugger, M. Fürstner, N. Vana, Y. Akatov, V. Shurshakov, and V. Arkhangelsky, "Dose distribution in the Russian Segment of the International Space Station," *Radiat. Prot. Dosim.*, vol. 120, pp. 446–449, 2006.

[12] G. Reitz, "Past and future application of solid-state detectors in manned spaceflight," *Radiat. Prot. Dosim.*, vol. 120, pp. 387–396, 2006.

[13] M. Casolino *et al.*, "The Altcriss project on board the International Space Station," *Adv. Space Res.*, vol. 40, pp. 1746–1753, 2007.

[14] L. Narici *et al.*, "The ALTE/ALTEINO projects: Studying functional effects of microgravity and cosmic radiation," *Adv. Space Res.*, vol. 33, pp. 1352–1357, 2004.

[15] G. Reitz and T. Berger, "The MATROSHKA Facility—History and science overview," in *36th COSPAR Scientific Assembly*, Beijing, China, Jul. 16–23, 2006.

[16] G. Reitz, "European dosimetry activities for the ISS," *Physica Medica*, vol. XVII, no. Supplement 1, 2001.

[17] T. Berger, "Radiation dosimetry onboard the International Space Station ISS," *Z Med. Phys.*, vol. 18, no. 4, pp. 265–275, 2008.

[18] G. Reitz, T. Berger, P. Bilski, R. Facius, M. Hajek, V. Petrov, M. Puchalska, D. Zhou, J. Bossler, Y. Akatov, V. Shurshakov, P. Olko, M. Ptaskiewicz, R. Bergmann, M. Fugger, N. Vana, R. Beaujean, S. Burmeister, D. Bartlett, L. Hager, J. Pálfalvi, J. Szabó, D. O'Sullivan, H. Kitamura, Y. Uchihori, N. Yasuda, A. Nagamatsu, H. Tawara, E. Benton, R. Gaza, S. McKeever, G. Sawakuchi, E. Yukihara, F. Cucinotta, E. Semones, N. Zapp, J. Miller, and J. Dettmann, "Astronaut's organ doses inferred from measurements in a human phantom outside the International Space Station," *Radiat. Res.*, vol. 171, pp. 225–235, 2009.

[19] J. Dettmann, G. Reitz, and G. Gianfiglio, "MATROSHKA-The first ESA external payload on the International Space Station," *Acta Astronautica*, vol. 60, no. 1, pp. 17–23, Jan. 2007.

[20] G. Reitz and T. Berger, "The MATROSHKA facility—Dose determination during an EVA," *Radiat. Prot. Dos.*, vol. 120, no. 1–4, pp. 442–445, 2006.

[21] Rando Phantom Lab, [Online]. Available: http://www.phantomlab.com/rando.html, 2008

[22] M. Hajek, V. Vana, and M. Fugger, Assessment of Radiation Exposure for Astronaut Crew During Spacewalks (Matroshka Experiment)—Austrian Results Univ. of Technology. Vienna, Austria, 2006.

[23] M. Hajek and R. Bergmann, "MATSIM: Data collection and planning," Atomic Inst., Vienna Univ. of Technol., Tech. Rep. MATSIM-WP2, 2008.

[24] A. Ferrari, P. R. Sala, A. Fasso, and J. Ranft, FLUKA: A Multi Particle Transport Code. Geneva, Switzerland, CERN, INFN, SLAC., 2005.

[25] V. Andersen *et al.*, "The application of FLUKA to dosimetry and radiation therapy," *Rad. Prot. Dos.*, vol. 116, no. 1–4, pp. 113–117, 2005.

[26] PTW Freiburg, Physikalisch-Technische Werkstätten, Dr. Pychlau GmbH,, Lörracher Strasse 7, 79115. Freiburg, Germany.

[27] T. W. Armstrong and B. L. Colborn, "Predictions of secondary neutron and proton fluxes induced in the International Space Station by the space radiation environment," SAIC Rep. 98042R, 1998.

[28] A. J. Tylka *et al.*, "CREME96: A revision of the cosmic ray effects on micro-electronics code," *IEEE Trans. Nucl. Sci.*, vol. 44, no. 6, pp. 2150–2160, Dec. 1997.

[29] NIST X-Ray Attenuation Database, [Online]. Available: http://www.nist.gov/physlab/data/xraycoef/index.cfm [Accessed: March 2010]